

A promising alternative to prediction of seasonal mean all India rainfall

Prince K. Xavier¹ and B. N. Goswami^{2,*}

¹Laboratoire de Meteorologie Dynamique, Ecole Normale Supérieure, Paris, France

²Indian Institute of Tropical Meteorology, Dr Homi Bhabha Road, Pashan, Pune 411 008, India

Prediction of seasonal mean All India Rainfall (AIR) is useful during extreme monsoon years (droughts and floods) when the rainfall anomaly is homogeneous over the country. It is, however, useless for any regional hydro-meteorological applications during 'normal' monsoon years (70 per cent of available record), when the rainfall anomaly is quite inhomogeneous within the country. Further, there exists an intrinsic limit to predict the seasonal mean monsoon. The theoretically achievable skill (with perfect model and near perfect data) for seasonal prediction of rainfall being barely useful, there is a need to explore an alternative strategy for monsoon prediction even if it is with a shorter lead time. Based on some of our previous work, we propose here that predicting the phases of the monsoon sub-seasonal oscillation (active and break spells) 3–4 weeks in advance is such an alternative strategy. We argue that such predictions would be more useful for regional hydro-meteorological applications. Potential for such extended range prediction is demonstrated. Using an empirical model, it is further demonstrated that this potential can be achieved and useful prediction of monsoon breaks three weeks in advance could be made. Future direction in improving such extended range prediction of sub-seasonal spells is discussed.

Keywords: All India rainfall, atmospheric general circulation model, seasonal mean.

The need and scope of prediction of seasonal mean monsoon rainfall

LARGE scale droughts and floods of the Indian summer monsoon (ISM) adversely affect country's agricultural production and economy and also cause immense property damage and human loss. Forewarning of seasonal mean rainfall is, therefore, demanded by the country's policy makers. As a result, for over a century, attempts have been made to predict the total summer monsoon rainfall using empirical techniques involving local and global antecedent parameters that correlate with the monsoon rainfall^{1–6}. The linear and nonlinear regression models as well as the neural network-based models⁷ perform reasonably well

when the monsoon is close to normal but fails to predict the extremes with useful skill. A case in point is the failure of almost all empirical models in predicting the drought⁸ of 2002. Another intrinsic limitation of the empirical techniques arises from interdecadal variation of the correlations between predictors and monsoon rainfall^{9–11}. Dynamical prediction of the seasonal mean monsoon using state-of-the-art climate models, therefore, offers a logical alternative to empirical forecasting. Unfortunately, the skill of prediction of the summer precipitation over the Asian monsoon region is currently negligible for almost all state-of-the-art atmospheric general circulation models (AGCM)^{12–16}. Multi-model super-ensemble forecasting^{17–20} shows some promise of improving the dynamical forecasts beyond the skill of individual models. However, the skill of such models also remains in the sub-useful range.

Reasons for AGCMs inability to predict the seasonal mean Indian monsoon rainfall

The inability of the state-of-the-art AGCMs in predicting the seasonal mean monsoon appears to be due to the following major factors.

First, even though AGCMs have improved over the last three decades in simulating the global climate in general, most models still have major systematic bias in simulating the seasonal mean ISM precipitation and its interannual variability (IAV)^{21–25}. Charney and Shukla²⁶ suggested that low frequency boundary forcing such as the tropical sea surface temperature (SST) variations predisposes the monsoon system toward a dry or a wet state. In other words, anomalous boundary conditions may provide potential predictability. For this to be true, models should be able to capture the interannual variability of the ISM. However, in reality, this is not the case as most models find the simulation of even the mean summer monsoon precipitation extremely difficult and have even greater difficulty in simulating the interannual variability of the ISM rainfall.

The predictable component of IAV of Indian summer monsoon comes from the teleconnection of Indian monsoon with slowly varying 'external' forcing such as the El Niño and Southern Oscillation (ENSO)²⁷. Simulation of the correct sign and amplitude of IAV of the monsoon by the AGCM depends on its ability to correctly simulate

*For correspondence. (e-mail: goswami@tropmet.res.in)

this teleconnection pattern. Almost all AGCMs have significant bias in simulating this teleconnection pattern. This is one contributing factor for the AGCMs inability to simulate the observed IAV of ISM.

A part of IAV of the ISM arises from local interaction between the warm pool over the eastern Indian Ocean (IO), Bay of Bengal and western Pacific and the atmosphere²⁸. This air–sea interaction leads to a negative correlation between SST and precipitation over the region while AGCMs forced with observed SST tend to simulate a positive correlation between precipitation and SST. Therefore, coupled GCMs (CGCMs) are essential for predicting the IAV of the ISM¹⁶. However, the current CGCMs also have large systematic biases in simulating the ISM, limiting their utility for predicting the seasonal mean ISM.

Finally, there appears to be an intrinsic limit on predictability of ISM due to the existence of significant ‘climate noise’ in this region. Following the seminal work of Charney and Shukla²⁶, even though it has been shown^{29–34} that the tropical climate is largely driven by anomalous boundary conditions and its simulation is much less sensitive to initial conditions, the ISM appears to be an exception within the tropics and its simulation seems to be quite sensitive to initial conditions^{24,35–37}. In the present study, the seasonal predictability of the ISM is examined using a fully atmosphere–ocean coupled GCM that has a realistic summer monsoon climatology.

The coupled model we use here has ECHAM4 as atmosphere component³⁸. The model equations are solved on 19 hybrid vertical levels (top at 10 hPa) by using the spectral transform method. Here ECHAM4 is used with a triangular truncation T42, which corresponds to an associated Gaussian grid of about $2.8 \times 2.8^\circ$ in latitude and longitude. The ocean model is similar to the one used by Météo-France, i.e. OPA 8.1. It is the ocean modelling system developed by the LODYC team in Paris³⁹. OPA is a finite difference OGCM and solves the primitive equations with a nonlinear equation of state on an Arakawa C-grid. The present configuration uses horizontal resolution of $1.5 \times 2^\circ$ in latitude and longitude with 0.5° latitudinal resolution close to the equator. There are 31 vertical levels with a rigid lid approximation.

The hindcasts are part of the DEMETER project⁴⁰. A nine member ensemble of 21 year hindcasts for the period 1981–2001 has been utilized to estimate the predictability of the ISM. Each hindcasts starts from 1 May initial conditions (9 members for each year). The total length of each hindcast is six months. The average rainfall during 1 June to 30 September is considered here as seasonal mean. This model has been chosen due to its rather realistic representation of the features of observed summer monsoon rainfall climatology (Figure 1). The observed rainfall data is taken from the CMAP (Climate Prediction Center Merged Analysis of Precipitation⁴¹) that is based on merging of gauge observations, satellite estimates and numerical model outputs. Most of the features of the seasonal

rainfall distribution over monsoon trough, western coast of India and the rainfall maxima over the eastern equatorial Indian Ocean are well simulated.

The model’s ability to correctly predict the observed IAV of the ISM, together with the analysis of the internal IAV (IIAV) and forced IAV (FIAV) in these hindcasts is examined using a rainfall index of monsoon. The Extended Indian Monsoon Rainfall (EIMR), defined as the average precipitation over the homogeneous region 70° – 100°E , 10° – 30°N ⁴² is used for this purpose. There is a relatively large spread amongst the ensemble members for most years (Figure 2) and somewhat less inter-member variability for some years (e.g. 1988, 1997). For most years however, there is hardly any correspondence with the observed EIMR (from CMAP). For example, in 1997, all model EIMR show low values while the observed rainfall is high. Thus, despite the ability of the model to depict the observed amplitude of IAV of the summer monsoon, it fails to predict the phases of observed IAV of ISM. This figure also illustrates the significant member to member variability in predicting the seasonal mean of ISM precipitation.

Is the poor skill of predictions of seasonal mean summer monsoon precipitation a systematic problem of the model or is it endemic to the ISM? To investigate this, it is essential to understand the components of interannual monsoon variability. The observed interannual variation

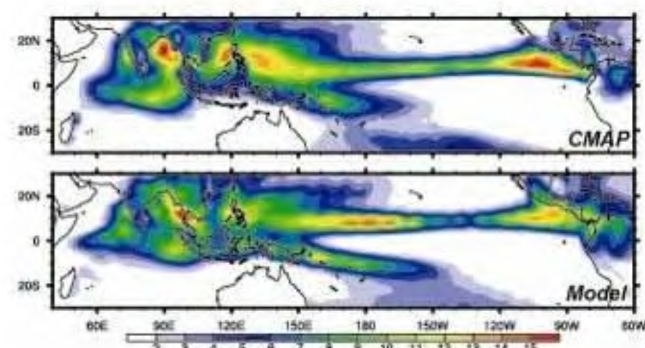


Figure 1. Climatological June–September (JJAS) averaged rainfall (mm day^{-1}).

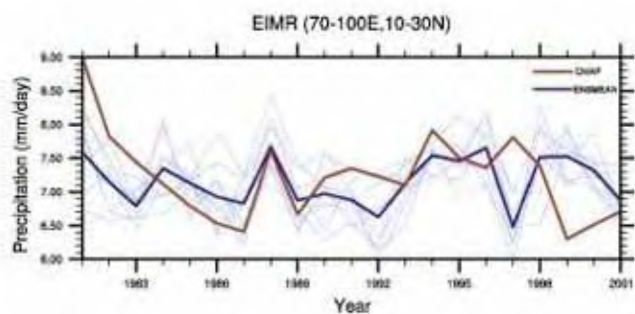


Figure 2. Ensemble evolution of JJAS precipitation averaged over the region 70° – 110°E , 10° – 30°N of each ensemble member (thin blue lines), the ensemble mean (thick blue line) and the observed values from CMAP (thick red line).

of the ISM is in fact made up of a 'forced' component and an 'internal' component. The observed time series is analogous to one simulated member. Since the statistics on the well-observed IAV is limited to around 21 years, it is difficult to extract a FIAV from the total IAV in the observed time series. Since we have only nine member hindcasts, the variance amongst the 21 ensemble means (i.e. FIAV) could still contain some influence of the IIAV. We, therefore, compare the total IAV with the IIAV⁴³ (Figure 3). The total IAV, which is a combination of FIAV and IIAV, is calculated as the variance of 189 (21 years \times 9 members) JJAS mean precipitation values. The ratio between total IAV and the IIAV from the hindcasts is shown in Figure 3. A ratio close to 2 (or less) represents regions where the IIAV is comparable to (or larger than) the FIAV. While the predictability of the summer precipitation over the equatorial Pacific may be significant, that over the ISM (north of 10°N) is marginal, where the internal variability appears to be the dominant factor. The conclusion on the role of internal variability over the ISM region derived from this model is nearly identical to that obtained by Goswami⁴⁴ using GFDL AGCM forced with observed monthly mean SST. There could be some influence of the model parameterization on the IIAV in the hindcasts. However, the result is consistent with findings of Kumar and others¹⁴ where they used a large number of AGCMs and found that the mean probability density function (PDF) of correlations between simulations and observations under perfect model scenario is about 0.7, indicating that only about 50% of the ISM variability is forced while the remaining 50% or more is internally driven.

What is responsible for the enhanced internal IAV over the Asian monsoon region? This internal variability has been shown to be generated by the vigorous intraseasonal oscillations over the monsoon regions⁴⁵ by virtue of the broad-band nature and the binomial character of rainfall time series⁴⁶. Therefore, the current generation of GCMs (coupled or uncoupled) need to be improved in simulating the intraseasonal variability and the associated air–sea interaction processes in order to be able to represent the observed 'climate noise' realistically. While these im-

provements demand better understanding of the physical processes, the future of seasonal prediction of the summer monsoon appears rather bleak.

Futility of prediction of seasonal mean All India Rainfall

As mentioned above, the empirical models as well as the dynamical models attempt to predict the area averaged rainfall over the continent (AIR). This is primarily because skill in predicting rainfall over smaller spatial scale is even poorer. The utility of forecasts of (averaged) all India summer monsoon rainfall to the user community, i.e. the agriculture and hydrological sector, remains uncertain. While the anomaly of seasonal mean rainfall has the same sign over most of the continent in extreme flood or drought years, it is rather inhomogeneous in 'normal' monsoon years (Figure 4). Therefore, it would be difficult even with a skillful forecast of the all India seasonal rainfall to provide regional communities with information that could be used effectively in agriculture and water resources management⁴⁷.

Need for an alternative approach

Thus, there not only exists an intrinsic limit to predicting the seasonal mean ISM, but such a forecast may not be of much use most of the time. Research efforts on seasonal prediction should continue so that dynamical models will be able to simulate and predict the extreme monsoon droughts and floods, when the accurate seasonal prediction is needed most. However, it is also important to explore an alternative strategy of extended range prediction even if with lead time less than a season.

We propose that skillful and timely forecast of the monsoon sub-seasonal variations (active-break spells) 3–4 weeks in advance would be more useful for regional agricultural and hydrological planning. Instead of the total quantum of rainfall for the whole season, prediction of active and weak spells would be more important for two reasons. (i) As sowing, harvesting and critical growth periods of most crops depend crucially on the timing of the dry and wet spells, the prediction of these spells even 2–3 weeks in advance will be of immense help. (ii) About 80 per cent of natural disasters are caused by extreme hydro-meteorological events (e.g. flash flood). These extreme rainfall events are modulated by intraseasonal variability^{48–50}. If we could provide useful forecast of the intraseasonal variability with lead-times of a few weeks, it will help the managements of weather-sensitive socioeconomic activities and reduce the damage caused by extreme events. Further, there may be higher scope of predicting the intraseasonal spells compared to that for predicting the interannual variation of the seasonal mean. This conjecture is based on the following observation.

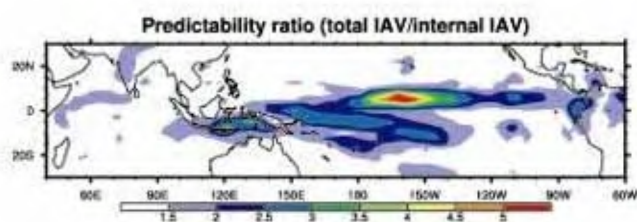


Figure 3. Predictability ratio defined as the ratio of total interannual variability (variance of 21 years and nine members) and the internal interannual variability (variance among members averaged over the years). Regions with values less than 2 are regions where the rainfall variability is mostly determined by the internal variability.

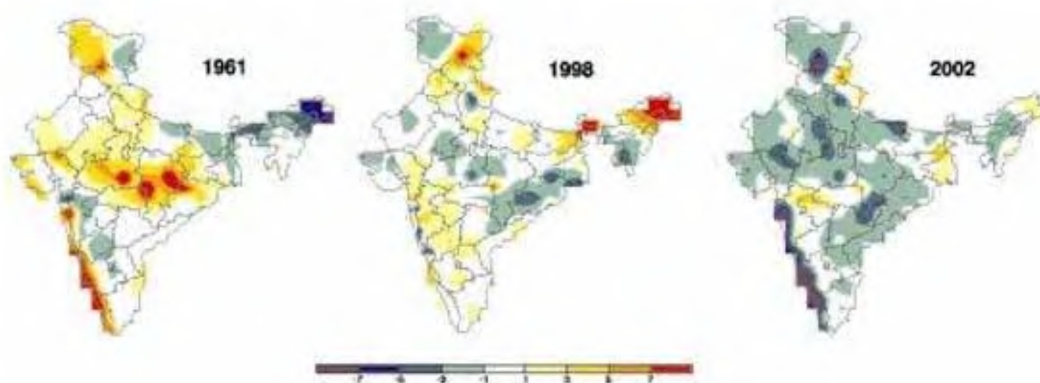


Figure 4. Anomalies of summer mean rainfall.

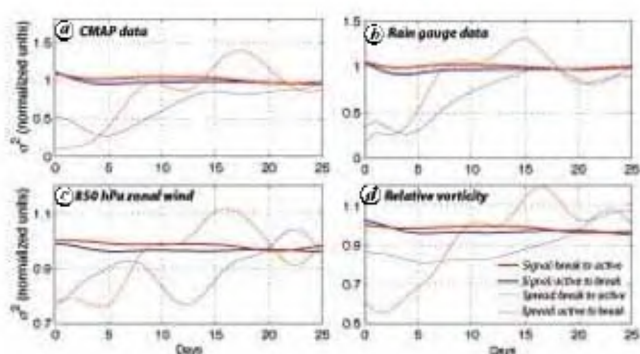


Figure 5. *a*, The thick red (blue) line is the monsoon ISO signal starting from troughs (peaks) of the index. The thin red (blue) line is the standard deviation (or spread) of different evolutions as a function of days from the initial date corresponding to all troughs (peaks) of the index representing transitions from break to active (active to break). *b*, Same as (*a*) but for high resolution gridded daily rain gauge data⁵³ for the JJAS season of 1951–2003, averaged over 70°–90°E, 18°–30°N. *c*, Same as (*a*) but for evolution of zonal wind at 850 hPa averaged over 80°–95°E, 12°–18°N. *d*, Same as (*a*) but for relative vorticity at 850 hPa averaged over the monsoon trough.

The signal of IAV of seasonal mean (s.d. of IAV of seasonal mean relative to long-term mean) is small (10 per cent) and could be difficult to untangle from ‘climate noise’. On the other hand, the signal of intraseasonal variability (ISV) (s.d. of ISV relative to long-term mean) is much larger (25–30 per cent) making it potentially separable from the noise. In addition, the ISV of the rainfall seems to be rather well tied up with oceanic variations (SST) and provides some memory of the subseasonal variation.

Intraseasonal predictability

In this section we briefly describe a method to estimate potential predictability of active and break phases of monsoon ISO from observations, based primarily on the work reported by Goswami and Xavier⁵¹. The method depends on the realization that if monsoon active and break were repeatable sinusoidal oscillations, they would be in-

initely predictable. The limit on predictability arises from the event-to-event variability of ISO as well as differences in evolution of the ISO from the same phase in different events. Therefore, divergence in evolutions from a given phase between different events may give us a measure of potential predictability of the monsoon ISO. We apply this idea on an observed index of monsoon ISO defined as the time series of CMAP⁵² rainfall anomalies (10–90 days band passed) averaged over 70°–90°E, 15°–25°N and normalized with its own standard deviation. Out of the 23 summer monsoon seasons considered here (1979–2002), 66 active and 63 break conditions are identified. Evolutions of the index for 25 days from all these active and break conditions are grouped separately and the spread in evolutions as measured by the standard deviation of these evolutions are shown in Figure 5. The limit on predictability is reached when the spread in evolutions become as large as the signal. Here the signal is the amplitude of the ISO, defined as the standard deviation of the filtered time series over a period comparable to the period of the ISO (taken as 50 days). The thick red (thick blue) line in Figure 5 *a* is the mean (averaged over all 66 or 63 events) signal starting from troughs (peaks). As expected, the signals starting from either troughs or peaks are close to each other. The spread becomes larger than the signal in eight days (20 days) for transitions from break to active (active to break). Thus, monsoon breaks are inherently more predictable than active conditions. Generally, a transition from an active (break) phase goes over to a break (active) phase within about 15–20 days. These results indicate that useful prediction of monsoon breaks could possibly be made up to about 20 days in advance while those for active conditions is likely to be limited to a lead time of about 10 days. This has been verified with a rainfall time series of high resolution gridded daily rain gauge data⁵³ for the JJAS season of 1951–2003, averaged over 70°–90°E, 18°–30°N (Figure 5 *b*).

Since the monsoon ISOs are convectively coupled phenomena, these fundamental differences in the predictability of active and break phases are evident in the circulation

parameters as well. 10–90 day filtered daily relative vorticity anomalies at 850 hPa level averaged over the monsoon trough (70°–90°E, 15°–25°N) is constructed from NCEP/NCAR reanalysis⁵⁴ for the same period (1979–2001). The vorticity time series is also normalized by its own standard deviation ($4.93 \times 10^{-6} \text{ s}^{-1}$). Spreads in evolution of normalized vorticity from active to break and from break to active, calculated using initial dates for active and break from the rainfall index (Figure 5 *d*), are similar to those for precipitation (Figure 5 *a*). Examination of the spread in transitions of an 850 hPa zonal wind index over 80°–95°E, 12°S–18°N also shows similar behaviour for divergence of evolutions for the two transitions (Figure 5 *c*).

What is responsible for the fundamental difference in divergence of trajectories from break to active as compared to that from active to break? As a result of this clustering of synoptic activity by the ISOs⁴⁹, the transition from break to active phase of monsoon ISO occurs through growth of gregarious convective activity and their organization while the transition from active to break represents the decay phase of organized convection, with far fewer growing convective elements. The growth of errors in the transition from break to active is, therefore, governed by fast growing convective instability while the growth of errors in the transitions from active to break is governed by the low frequency 30–60 day oscillations of the monsoon Hadley circulation⁵⁵.

A real-time prediction strategy

The observed regularities in the evolutions and the similarities in the large-scale spatial patterns of monsoon ISOs have motivated us to attempt an analogue method for extended range monsoon forecasting. Even though one cannot expect exactly identical analogues, as the weather hardly repeats, it should be possible to find closely matching analogues of the large-scale envelope of monsoon intraseasonal variability. The success of the forecasts would depend on the number of such analogues one can isolate from the data. Hence, the constraints for choosing a variable for forecasting must be a reasonably long history observation as well as its availability on real-time. One such variable that bears close association with the rainfall is the OLR. We choose NOAA interpolated OLR⁵⁶ as it meets these criteria.

We assume that the predictable component of the sub-seasonal variations is the large-scale envelope of intraseasonal oscillations that contain high frequency weather fluctuations embedded on it. It is indeed a difficult task to predict the day-to-day weather variations 15–25 days in advance. To highlight the low frequency intraseasonal variations and to smoothen the high frequency synoptic weather variations, the NOAA interpolated daily OLR data are converted into 5 day averages (pentad means). The

model we propose is to predict the intraseasonal variations of pentad averaged data. The total data length is divided into two segments, namely a 21-year modelling period (1 January 1979–31 December 1999) and a nearly 6-year hindcast period (1 January 2000–29 August 2005). Pentad OLR data till the beginning of the hindcast period (say $t = t_0$; here, 1 January 2000) is subjected to EOF decomposition⁵⁷ into a number of spatial and temporal modes. EOF decomposition is performed over the domain 50°–110°E, 15°S–30°N as this area represents the maximum sub-seasonal variability during the summer monsoon season. The first 10 modes contribute about 75% of the total variance. Higher modes may be considered as noise. A second step to filter out the noise from the data is by reconstructing the OLR data with the first 10 EOFs and PCs as

$$\text{OLR}_r(x, y, t) = \sum_{n=1}^{10} \text{EOF}_n(x, y) \times \text{PC}_n(t), \quad (1)$$

where $\text{OLR}_r(x, y, t)$ is the reconstructed OLR, $\text{EOF}_n(x, y)$ and $\text{PC}_n(t)$ the n th EOF and PC respectively. Ten EOFs are chosen as a compromise between maximizing the amount of variance for the reconstructed OLR data and minimizing the noise in the form of higher modes. The seasonal cycle of OLR is retained in the modelling data and therefore the predictions will also contain the seasonal cycle. However, the presence of winter season in the modelling data will not affect predictions of summer values due to the intrinsic property of analogue method that automatically identifies suitable analogues from the corresponding season. This feature is highly advantageous for operational forecasting purposes as it requires minimum data processing efforts. The details of the analogue model and evaluation of its skill in hindcasts are presented in detail by Xavier and Goswami⁵⁸. A brief summary is presented here.

1. Consider the spatial pattern of t_0 and find the spatial correlation (in the domain 50°–110°E, 15°S–30°N) with the spatial patterns at each time step in the modelling period.
2. Find the spatial root mean square error (RMSE) between spatial pattern of t_0 and the spatial patterns at each time step in the modelling period.
3. Check whether the spatial correlations are above 0.7 and spatial RMSE less than 20 W m^{-2} . These values are arbitrarily chosen, so as to have enough number of analogues. Those patterns satisfying this criterion are considered as the spatial analogues of t_0 . Let them be p_i , $i = 1, 2, \dots, N$, where N is the number of spatial analogues found. Typical values of N are around 55.
4. Consider the evolution of PC1 from t_0-5 to t_0 and find the temporal correlation and RMSE between the PC1 from p_i-5 to p_i , $i = 1, 2, \dots, N$. If the correlations are

greater than 0.5 (arbitrary, yet gives enough number of analogues) and RMSE less than unit standard deviation of PC1, then those are the temporal analogues of PC1 from t_0-5 to t_0 . Let them be q_j , $j = 1, 2, \dots, M$, where M is the number of temporal analogues (typically of the order of 20) of PC1 and $M = N$.

5. Forecasts of PC1 at lead time τ pentads are generated as

$$PC1(t_0 + \tau) = \frac{1}{M} \sum_{j=1}^M PC1(q_j + \tau). \quad (2)$$

6. Repeat steps 4–5 for PC2, PC3, ..., PC10. Then we have the predicted values of each PC as $PC_k(t_0 + \tau)$, $k = 1, 2, \dots, K$, where K is the number of EOFs used. Here $K = 10$.

7. Predicted OLR values for lead time τ are generated as

$$OLR(x, y, t + \tau) = \sum_{k=1}^K EOF_k(x, y) \times PC_k(t_0 + \tau). \quad (3)$$

No forecast is possible if $N = 0$ or $M = 0$. Such time steps are considered as unpredictable by this method. However, with the correlations and RMSE criteria used here, no such unpredictable time steps are found during the hind-cast period. Since our interest is in predicting the intraseasonal variations embedded on the annual cycle and in order to eliminate any artifacts due to the apparent skill in predicting the annual cycle, the intraseasonal anomalies are extracted from the total OLR predictions and the corresponding observations by removing the corresponding climatological annual cycle. The predictions are scaled by a factor determined by the ratio of variance explained by the first 10 EOFs to the total OLR variance. Hereafter, all the results presented are based on the intraseasonal OLR anomalies computed as described above.

A few important features of the predictions are highlighted here. Predictions are significantly skillful up to 5 pentads in advance (Figure 6a). There are differences in predictability of ISV depending on the initial condition from where the forecasts are made^{51–59}. This property has been verified here by selecting a number of active and break conditions using a normalized index OLR over central India. Dates when the normalized OLR value below -1.0 is considered as active condition and when it is above $+1.0$ as break. Forecasts made from these active and break initial conditions are compared with the corresponding observations and the correlations over the number of active and break states are given in Figure 6b. Supporting the findings of Goswami and Xavier⁵¹, we find that the forecasts starting from an active monsoon initial condition remain skillful even up to 5 pentads, while those starting from a break like initial state show useful skills only up to 2–3 pentads. Generally, an active condition evolves into a monsoon break in about 20 days

and the results indicate higher predictability of break conditions (initialized from an active state).

4 pentad lead predictions of OLR variations over central India (Figure 7a) show that most of the large intraseasonal convection variability is forecasted fairly well. A case in point is the fairly accurate predictions of the long mid-season break of 2002 that resulted in the unprecedented drought over the country. Another important utility of this forecasting strategy is to generate predictions for smaller regions (or regional scale forecasts). Regional forecasts made for six regions of the country indicate high skills for the central and western Indian regions (Figure 7b).

Conclusion and discussions

While prediction of seasonal mean all India rainfall may be useful in getting an outlook of the agricultural production of the country as a whole, it is not useful for individual farmers as the rainfall anomaly is highly inhomogeneous over the country during ‘normal’ monsoon years. Further, due to existence of significant ‘climate noise’ in the region, the skill of prediction of seasonal mean Indian summer monsoon may remain poor. Thus, there is a profound need for an alternative strategy to prediction of seasonal mean AIR.

The prediction of the active and break spells of monsoon 2–3 weeks in advance is proposed as such an alternative strategy here. First, the physical basis for such a prediction strategy is established from the calculation of potential predictability of monsoon ISOs. Then, an ana-

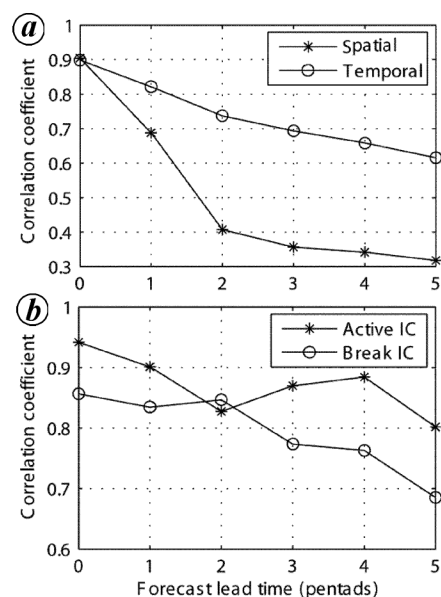


Figure 6. a, Spatial and temporal correlations between observations and predictions over Central India at different lead times. b, Temporal correlations between predictions and observations from active and break initial conditions at different lead times.

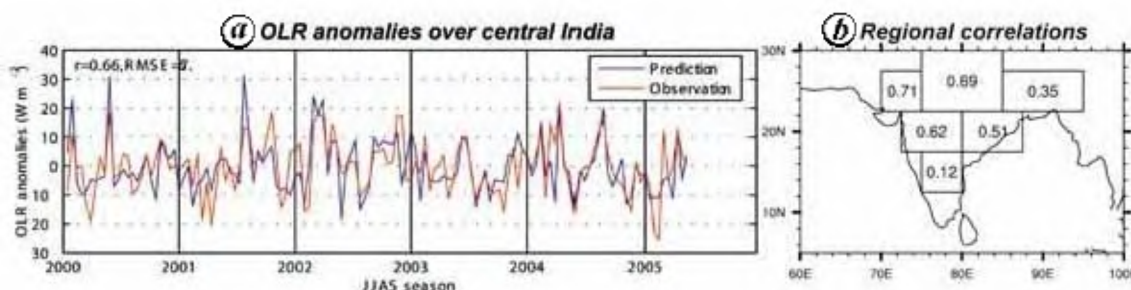


Figure 7. *a*, Prediction of OLR anomalies (W m^{-2}) at 4 pentad lead in comparison with observed values over the region 75° – 95°E , 20° – 25°N for the JJAS season of the hindcast period. *b*, The correlation coefficient between 4 pentad lead predictions and observations averaged over these regions for the JJAS period.

logue technique is proposed and its skill in predicting the active and break spells 2–3 weeks in advance is demonstrated. This model has great potential for real time prediction as it does not suffer from the so-called ‘end point’ problem. Moreover, it is demonstrated that the model has skill in predicting the monsoon ISOs on smaller regional scales.

The success of the simple empirical model presented here in predicting the phases of monsoon sub-seasonal oscillations three weeks in advance is noteworthy. This is a simple linear technique. However, the probability distribution function of the higher frequency component of monsoon sub-seasonal oscillations (e.g. 10–20 day mode) appears to indicate nonlinearity. Therefore, a judicious combination of linear and nonlinear time series prediction techniques may yield improved prediction of the active–break phases. Such a technique was successfully used to produce improved seasonal prediction of AIR³.

Dynamically, coupled ocean–atmosphere models must be used to predict the monsoon subseasonal oscillations as it is now established that they are associated with ocean–atmosphere interactions. However, two major problems have kept the skill of any such coupled model in predicting the monsoon sub-seasonal oscillations at a very low level. The first problem is related to the fact that most coupled models have large systematic bias in simulating the statistics of observed summer ISOs. The second one is more fundamental. The sub-seasonal oscillations have very large spatial scale and initial error in describing them is generally quite small while the small spatial scales are not well represented in the initial condition. Rapid growth of errors in small scales (in any such models) and nonlinear cascading of these errors to the larger ISO scale makes the errors in the ISO scale very large in a relatively short time. This essentially makes it difficult to predict them. If, however, some method of initialization could be evolved to prevent this nonlinear cascading of errors, dynamical models will be able to produce useful forecasts of sub-seasonal phases.

1. Blanford, H. F., On the connection of the Himalaya snowfall with dry winds and seasons of drought in India. *Proc. R. Soc. London*, 1884, **37**, 3–22.

2. Gowarikar, V., Thapliyal, V., Sarker, R. P., Mandel, G. S. and Sikka, D. R., Parametric and power regression models: new approach to long range forecasting of monsoon rain in India. *Mausam*, 1989, **40**, 125–130.
3. Iyengar, R. N. and Kanth, S. T. G. R., Intrinsic mode functions and a strategy for forecasting Indian monsoon rainfall. *Meteorol. Atmos. Phys.*, 2005, **90**, 17–36.
4. Sahai, A. K., Grimm, A. M., Satyan, V. and Pant, G. B., Long-lead prediction of Indian summer monsoon rainfall from global SST evolution. *Climate Dyn.*, 2003, **20**(7/8), 855–863.
5. Walker, G. T., Correlation in seasonal variations of weather. iii: A preliminary study of world weather. *Mem. Indian Meteorol. Dept.*, 1923, **24**, 75–131.
6. Walker, G. T., Correlation in seasonal variations of weather. iv: A further study of world weather. *Mem. Indian Meteorol. Dept.*, 1924, **24**, 275–332.
7. Goswami, P. and Srividya, A novel neural network design for long-range prediction of rainfall pattern. *Curr. Sci.*, 1996, **70**, 447–457.
8. Gadgil, S., Srinivasan, J., Nanjundiah, R. S., Kumar, K. K., Munot, A. A. and Kumar, K. R., On forecasting the Indian summer monsoon: the intriguing season of 2002. *Curr. Sci.*, 2002, **83**, 394–403.
9. Kriplani, R. H. and Kulkarni, A., Climate impact of El Nino/La Nina on the Indian monsoon: A new perspective. *Weather*, 1997, **52**, 39–46.
10. Krishnamurthy, V. and Goswami, B. N., Indian monsoon–enso relationship on inter decadal time scales. *J. Climate*, 2000, **13**, 579–595.
11. Kumar, K. K., Rajagopalan, B. and Cane, M. A., On the weakening relationship between the Indian monsoon and ENSO. *Science*, 1999, **284**, 2156–2159.
12. Kang, I. S., Lee, J. Y. and Park, C. K., Potential predictability of summer mean precipitation in a dynamical seasonal prediction system with systematic error correction. *J. Climate*, 2004, **17**, 834–844.
13. Kang, I.-S. and Shukla, J., Dynamical seasonal prediction and predictability. In *The Asian Monsoon* (ed. Wang, B.), Springer, Heidelberg, 2006.
14. Kumar, K. K., Hoerling, M. and Rajagopalan, B., Advancing dynamical prediction of Indian monsoon rainfall. *Geophys. Res. Lett.*, 2005, **32**, L08704, doi:10.1029/2004GL021979.
15. Rajeevan, M., Pai, D. S., Dikshit, S. K. and Kelkar, R. R., IMD’s new operational models for long-range forecast of southwest monsoon rainfall over India and their verification for 2003. *Curr. Sci.*, 2004, **86**, 422–431.
16. Wang, B., Ding, Q., Fu, X., Kang, I.-S., Jin, K., Shukla, J. and Doblas-Reyes, F., Fundamental challenge in simulation and prediction of summer monsoon rainfall. *Geophys. Res. Lett.*, 2005, **32**, L15711, doi:10.1029/2005GL022734.

17. Krishnamurti, T. N. *et al.*, Multimodel superensemble forecasts for weather and seasonal climate. *J. Climate*, 2000, **13**, 4196–4216.
18. Krishnamurti, T. N. *et al.*, Improved weather and seasonal climate forecasts from multimodel superensemble. *Science*, 1999, **285**, 1548–1550.
19. Krishnamurti, T. N., Mitra, A. K., Kumar, T. S. V. V., Yun, W. T. and Dewar, W. K., Seasonal climate forecasts of the South Asian monsoon using multiple coupled models. *Tellus*, 2006, **58**, 487–507.
20. Krishnamurti, T. N. *et al.*, Real-time multianalysis-multimodel superensemble forecasts of precipitation using trmm and ssm/i products. *Mon. Weather Rev.*, 2001, **129**, 2861–2883.
21. Gadgil, S. and Sajani, S., Monsoon precipitation in the AMIP runs. *Climate Dyn.*, 1998, **14**, 659–689.
22. Kang, I.-S. *et al.*, Intercomparison of atmospheric GCM simulated anomalies associated with the 1997–98 El Niño. *J. Climate*, 2002, **15**, 2791–2805.
23. Saji, N. H. and Goswami, B. N., An intercomparison of the seasonal cycle of tropical surface stress simulated by 17 AMIP GCMs. *Climate Dyn.*, 1997, **13**, 561–585.
24. Sperber, K. R. and Palmer, T. N., Interannual tropical rainfall variability in general circulation model simulations associated with Atmospheric Model Intercomparison Project. *J. Climate*, 1996, **9**, 2727–2750.
25. Wang, B., Kang, I.-S. and Lee, J.-Y., Ensemble simulations of Asian–Australian monsoon variability by 11 AGCMs. *J. Climate*, 2004, **17**, 699–710.
26. Charney, J. G. and Shukla, J., Predictability of monsoons. In *Monsoon Dynamics* (eds Lighthill, J. and Pearce, R. P.), Cambridge University Press, Cambridge, 1981, pp. 99–108.
27. Goswami, B. N., Wu, G. and Yasunari, T., Annual cycle, intraseasonal oscillations and roadblock to seasonal predictability of the Asian summer monsoon. *J. Climate*, 2006, **19**, 5078–5099.
28. Wang, B., Wu, R. and Li, T., Atmosphere–warm ocean interaction and its impacts on Asian–Australian monsoon variation. *J. Climate*, 2003, **16**, 1195–1211.
29. Anderson, J. L. H., van den Dool, Barnston, A., Chen, W., Stern, W. and Ploshay, J., Present day capabilities of numerical and statistical models for atmospheric extratropical seasonal simulation and prediction. *Bull. Am. Meteorol. Soc.*, 1999, **80**, 1349–1361.
30. Fennessy, M. J. and Shukla, J., Impact of initial soil wetness on seasonal atmospheric prediction. *J. Climate*, 1999, **12**, 3167–3180.
31. Kumar, A. and Hoerling, M. P., Prospects and limitations of atmospheric GCM climate predictions. *Bull. Am. Meteorol. Soc.*, 1995, **76**, 335–345.
32. Lau, N. C., Modelling the seasonal dependence of atmospheric response to observed El Niño in 1962–76. *Mon. Weather Rev.*, 1985, **113**, 1970–1996.
33. Shukla, J., Predictability in the midst of chaos: A scientific basis for climate forecasting. *Science*, 1998, **282**, 728–731.
34. Shukla, J. and Wallace, J. M., Numerical simulation of the atmospheric response to equatorial Pacific sea surface temperature anomalies. *J. Atmos. Sci.*, 1983, **40**, 1613–1630.
35. Cherchi, A. and Navarra, A., Reproducibility and predictability of Asian summer monsoon in the ECHAM4-GCM. *Climate Dyn.*, 2003, **20**, 365–379.
36. Krishnamurthy, V. and Shukla, J., Intraseasonal and interannual variability of rainfall over India. *J. Climate*, 2000, **13**, 4366–4377.
37. Sperber, K. R., Slingo, J. M. and Annamalai, H., Predictability and the relationship between subseasonal and interannual variability during the Asian summer monsoons. *Q. J. R. Meteorol. Soc.*, 2000, **126**, 2545–2574.
38. Roeckner, E., The atmospheric general circulation model ECHAM-4: model description and simulation of present-day climate. Max-Planck-Institut für Meteorologie, Hamburg, Germany, 1996, Rep. No. 218.
39. Madec, G., Delecluse, P., Imbard, M. and Levy, C., OPA version 8.1 ocean general circulation model reference manual. LODYC/IPSL, Paris, France, 1998, pp. 11.
40. Palmer, T. N. *et al.*, Development of a European Multimodel Ensemble System for seasonal-to-interannual prediction (DEMETER). *Bull. Am. Meteorol. Soc.*, 2004, DOI: 10.1175/BAMS-85-6-853.
41. Xie, P. and Arkin, P. A., Global precipitation: A 17-year monthly analysis based on gauge observations, satellite estimates and numerical model outputs. *Bull. Am. Meteorol. Soc.*, 1997, **78**, 2539–2558.
42. Goswami, B. N., Krishnamurthy, V. and Annamalai, H., A broad-scale circulation index for interannual variability of the Indian summer monsoon. *Q. J. R. Meteorol. Soc.*, 1999, **125**, 611–633.
43. Rowell, D. P., Assessing potential seasonal predictability with an ensemble of multidecadal GCM simulations. *J. Climate*, 1998, **11**, 109–120.
44. Goswami, B. N., Interannual variations of Indian summer monsoon in a gcm: External conditions versus internal feedbacks. *J. Climate*, 1998, **11**, 501–522.
45. Goswami, B. N., South Asian monsoon. In *Intraseasonal Variability in the Atmosphere–Ocean Climate System* (eds Lau, K. and Waliser, D.), Praxis, Springer, 2005, pp. 19–61.
46. Goswami, B. N. and Xavier, P. K., Dynamics of ‘internal’ interannual variability of the Indian summer monsoon in a GCM. *J. Geophys. Res.*, 2005, **110**, doi:10.1029/2005JD006042.
47. Webster, P. J. and Hoyos, C., Prediction of monsoon rainfall and river discharge on 15–30-day time scales. *Bull. Am. Meteorol. Soc.*, 2004, **85**, 1745–1767.
48. Goswami, B. N. and Ajayamohan, R. S., Intraseasonal oscillations and interannual variability of the Indian summer monsoon. *J. Climate*, 2001, **14**, 1180–1198.
49. Goswami, B. N., Ajayamohan, R. S., Xavier, P. K. and Sengupta, D., Clustering of low pressure systems during the Indian summer monsoon by intraseasonal oscillations. *Geophys. Res. Lett.*, 2003, **30**(8), doi:10.1029/2002GL016734.
50. Jones, C., Waliser, D. E., Lau, K. M. and Stern, W., Global occurrences of extreme precipitation events and the Madden–Julian oscillation: Observations and predictability. *J. Climate*, 2004, **17**, 4575–4589.
51. Goswami, B. N. and Xavier, P. K., Potential predictability and extended range prediction of Indian summer monsoon breaks. *Geophys. Res. Lett.*, 2003, **30**(18), doi:10.1029/2003GL017810.
52. Xie, P. and Arkin, P. A., Analyses of global monthly precipitation using gauge observations, satellite estimates and numerical predictions. *J. Climate*, 1996, **9**, 840–858.
53. Rajeevan, M., Bhat, J. and Kale, J. D., A high resolution daily gridded rainfall data for the Indian region: Analysis of break and active monsoon spells. *Curr. Sci.*, 2006, **91**, 296–306.
54. Kalnay, E. *et al.*, The NCEP/NCAR 40-year reanalysis project. *Bull. Am. Meteorol. Soc.*, 1996, **77**, 437–471.
55. Goswami, B. N. and Shukla, J., Quasi-periodic oscillations in a symmetric general circulation model. *J. Atmos. Sci.*, 1984, **41**, 20–37.
56. Liebmann, B. and Smith, C. A., Description of a complete (interpolated) outgoing longwave radiation dataset. *Bull. Am. Meteorol. Soc.*, 1996, **77**, 1275–1277.
57. Björnsson, H. and Venegas, S., *A Manual for EOF and SVD Analyses of Climate Data*, McGill University, CCGCR Report No. 1997, 97–1.
58. Xavier, P. K. and Goswami, B. N., An analogue method for real-time forecasting of summer monsoon sub-seasonal variability. *Mon. Weather Rev.*, 2007, **135** (in press).
59. Waliser, D. E., Stern, W., Schubert, S. and Lau, K. M., Dynamic predictability of intraseasonal variability associated with the Asian summer monsoon. *Q. J. R. Meteorol. Soc.*, 2003, **129**, 2897–2925.